be an useful tool to predict the iron phase change and the optimized reacting conditions, i.e., critical flow rate, temperature and pressure, during the course of a F-T synthesis.

It was reported that the solubility of F-T reaction products (CO_2, H_2O, and hydrocarbons) are higher by about a factor of ten than that of CO and H_2 in wax for F-T synthesis; however, the solubility of CO and H_2 increases remarkably with temperature in contrast to the products gases whose solubility decreases with increases of temperature. By knowing the partial pressures of the gases in gas phase and assuming that the vapor and liquid are in equilibrium, the solubility of each gas can be calculated by using the data reported in the literature. The total amount of each compound in the gas and liquid phase can then be calculated and is shown in Figure 17. This figure, showing both gas and liquid phase compounds, is similar to the results shown in figure 15, which represents the gas phase only. Phase diagrams with the gas phase components are good enough to predict the phase change of iron and the reaction conditions of F-T synthesis.

D.4. Obtain Data on Rates Involved in the Interconversion of Iron Oxide and Carbide

No scheduled or additional activity to report.

D.5. Schedule of Activities for Next Quarter

- Continue efforts to improve our ability to remove wax from reactor with high-alpha Fe catalysts.

Table 1 Product Selectivities for 100Fe/4.4Si/2.6Cu/5.2K	
Conversion/%	
CO	68
H_2	58
CO + H_2	64
Productivity	
g HC Nm^{-3}-syngas feed	138
g HC g(Fe)	0.42
Water-Gas Shift	
$[CO_2][H_2O]/\{[CO][H_2]\}$	11
H_2:CO Usage	0.60
CO_2/mol%	45
Selectivity/Wt.%	
CH_4	2.2
C_2-C_4 (alkene %)	10.7 (77)
C_5-C_{11}	14.7 (78)
C_{12}+	72.4
C_2 (1-alkene %)	3.2 (78)
C_3	4.6 (74)
C_4	2.8 (75)
C_5	2.5 (68)
C_6	2.1 (72)
C_7	2.0 (77)
C_8	2.0 (77)
C_9	2.1 (75)
C_{10}	2.0 (71)
C_{11}	2.0 (76)

Table 2

Gas Phase Compositions

H_2 (psi)	CO (psi)	H_2O (psi)	CO_2 (psi)	C_4H_y (psi)	y	X, CO (%)	X, H_2 (%)	CO+H_2 (NL/hr)
25.4	26.7	4	78	55	8.63	0.86	0.8	15.9
32	43	6	72	36	8.52	0.78	0.76	21
39.4	60.1	8.49	61.1	20.154	8.48	0.685	0.692	31.3
50.3	89.5	10.7	32.6	5.27	8.44	0.46	0.54	63.1
54.8	102.4	10.3	18.8	3.14	8.43	0.32	0.45	91.6
59.24	107.3	9.23	11.8	1.82	8.36	0.23	0.37	126.2

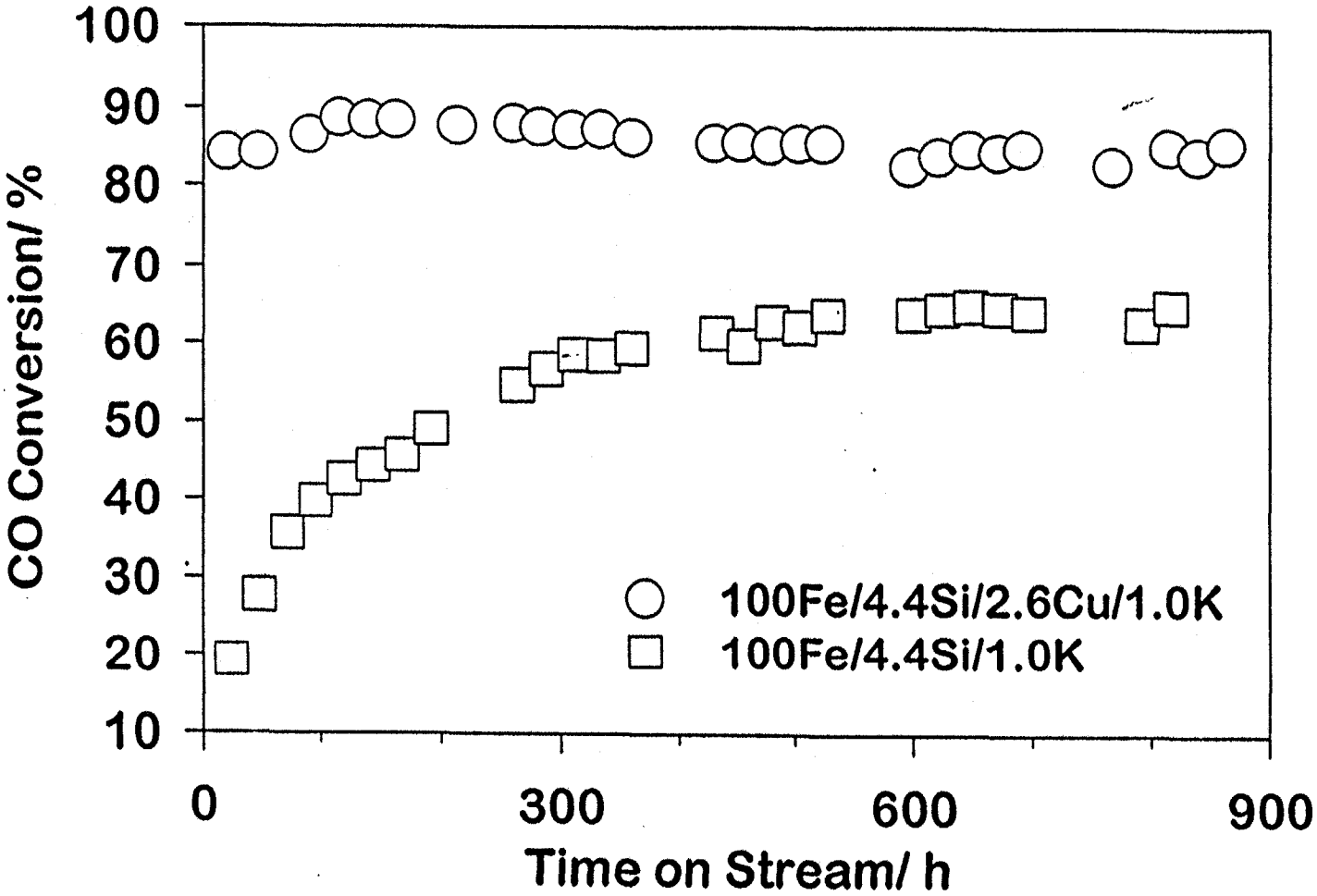

Figure 1. Affect of copper on carbon monoxide conversion for catalysts activated with hydrogen at 220°C, 0.10 MPa for 24 h.

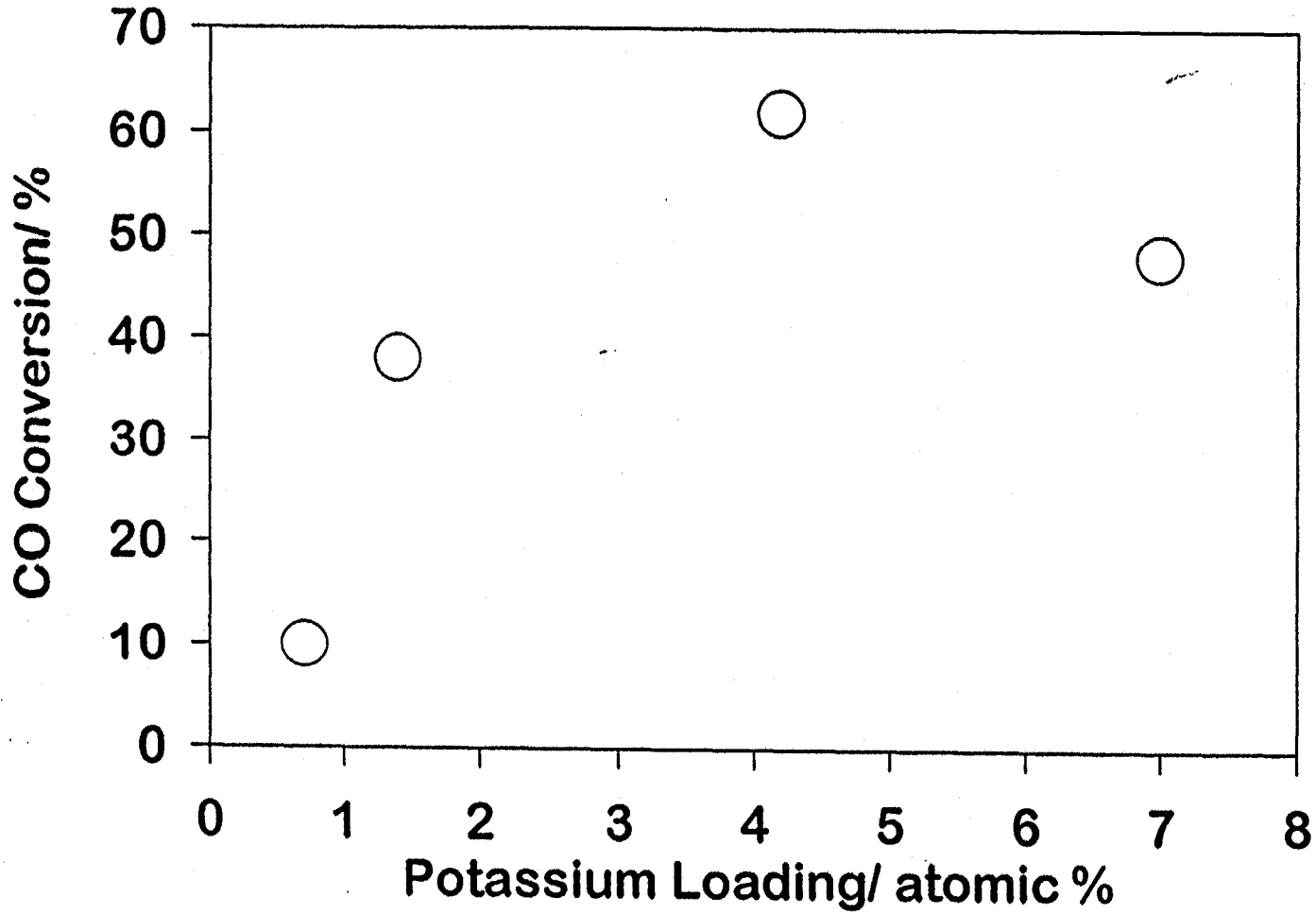

Figure 2. CO conversion as a function of potassium loading on a precipitated Fe-Si catalyst. H_2:CO=0.7, s.v.=0.75 NL h^{-1} g(Fe)$^{-1}$, 230^{o}C, 1.3 MPa.

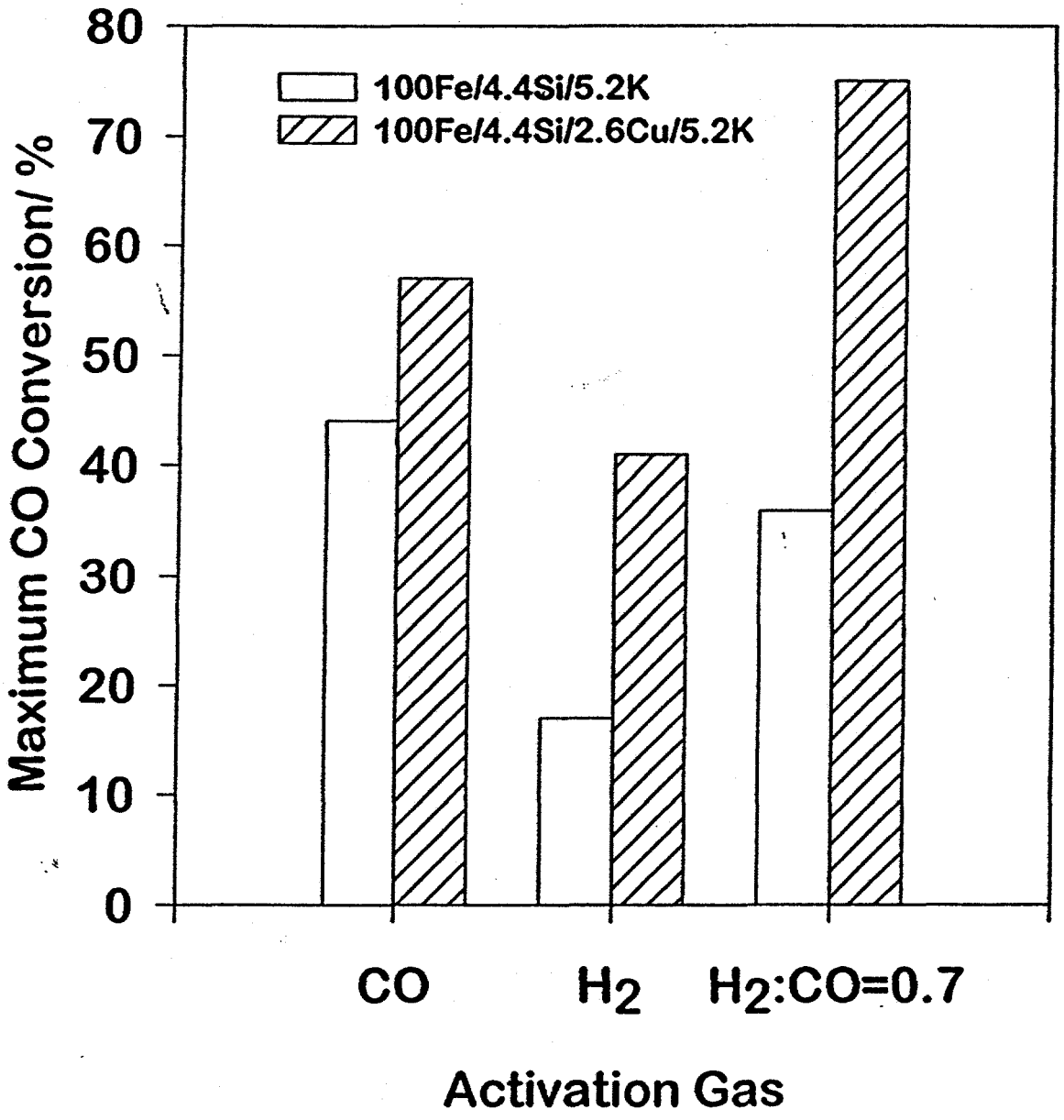

Figure 3. Affect of copper and activation gas on carbon monoxide conversion for precipitated iron-silicon catalyst at 230°C.

Figure 4. Conversion of CO_2 and CO during FTS at 270°C, 8 atm. and the flows indicated in the text.

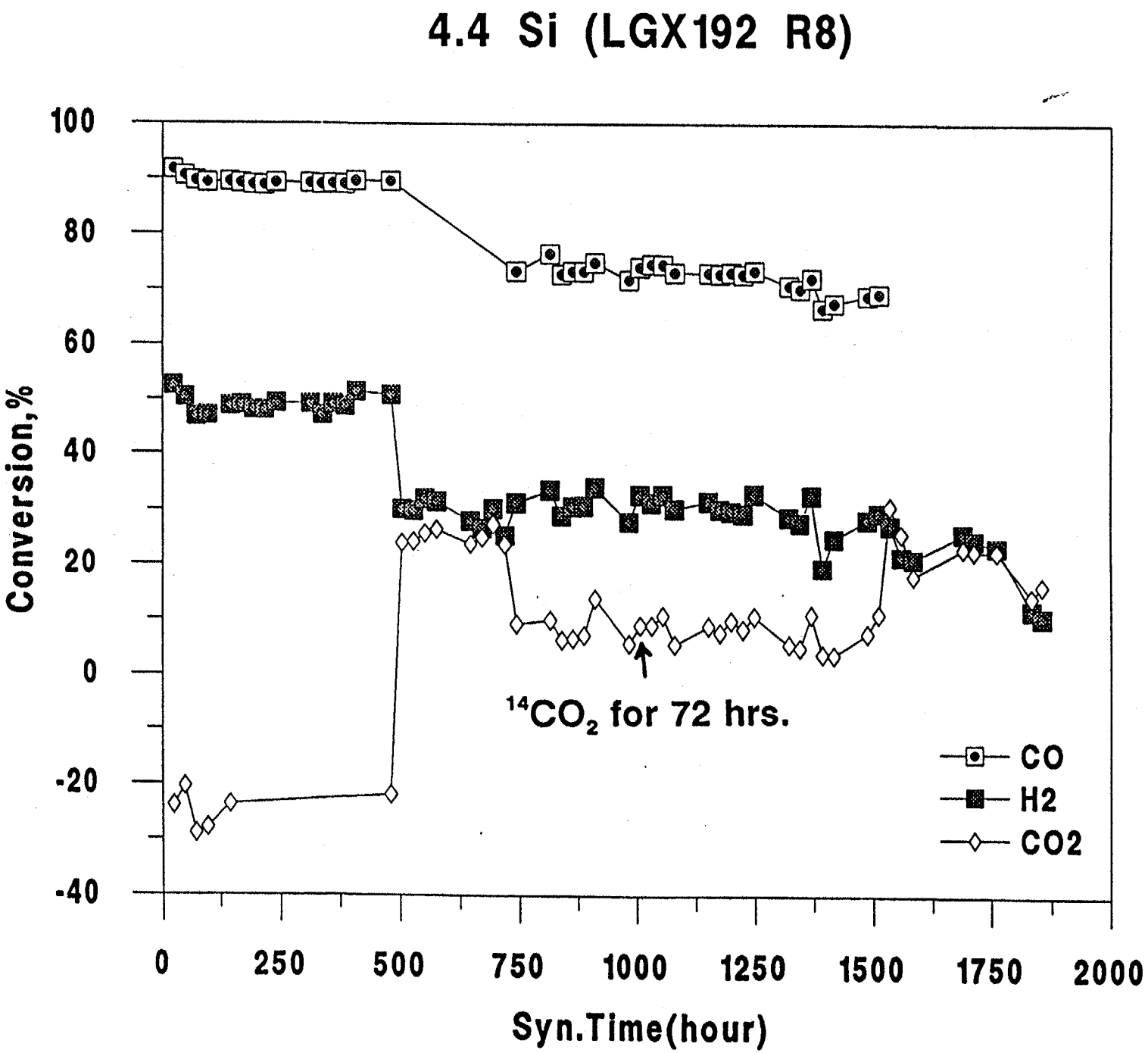

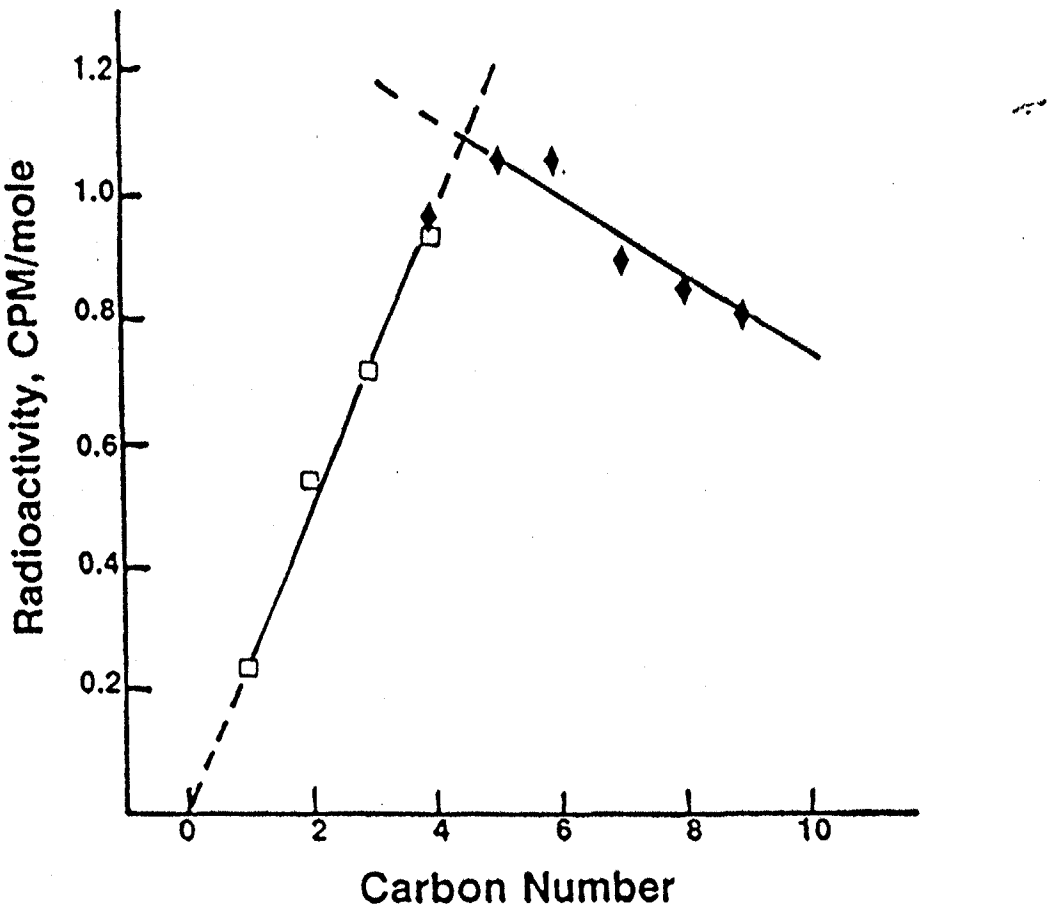

Figure 5. Radioactivity/mole for products generated while adding $^{14}CO_2$ (see text for conditions).

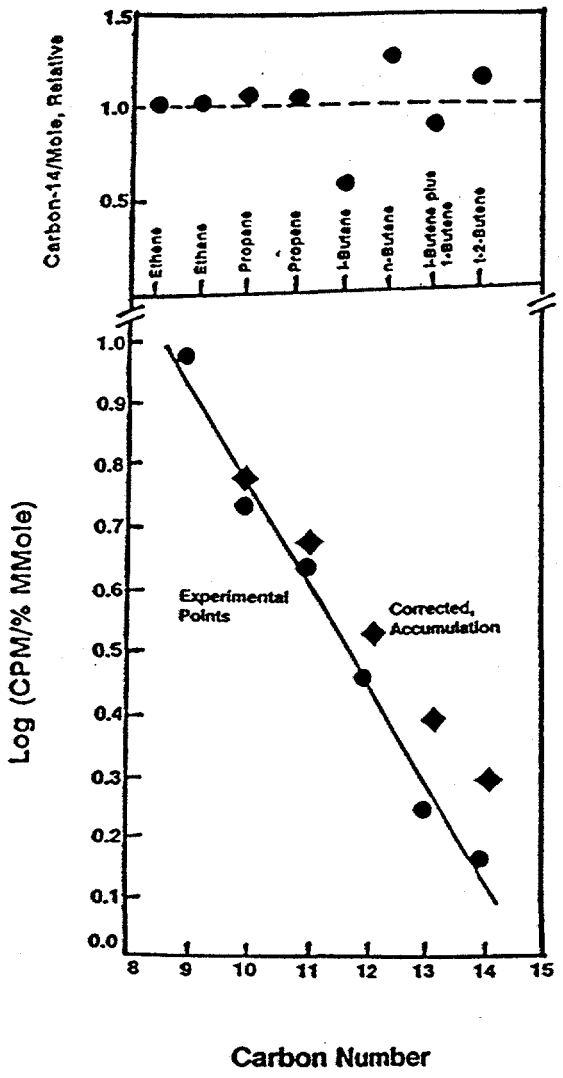

Figure 6. Composite figure showing relative radioactivity for the lower carbon number compounds (●); the measured values for the higher carbon number compounds (●), and the values for the higher carbon number compounds (◆) after correcting for reactor accumulation effects.

Figure 7. Phase diagram at 15 atm. and 300°C.

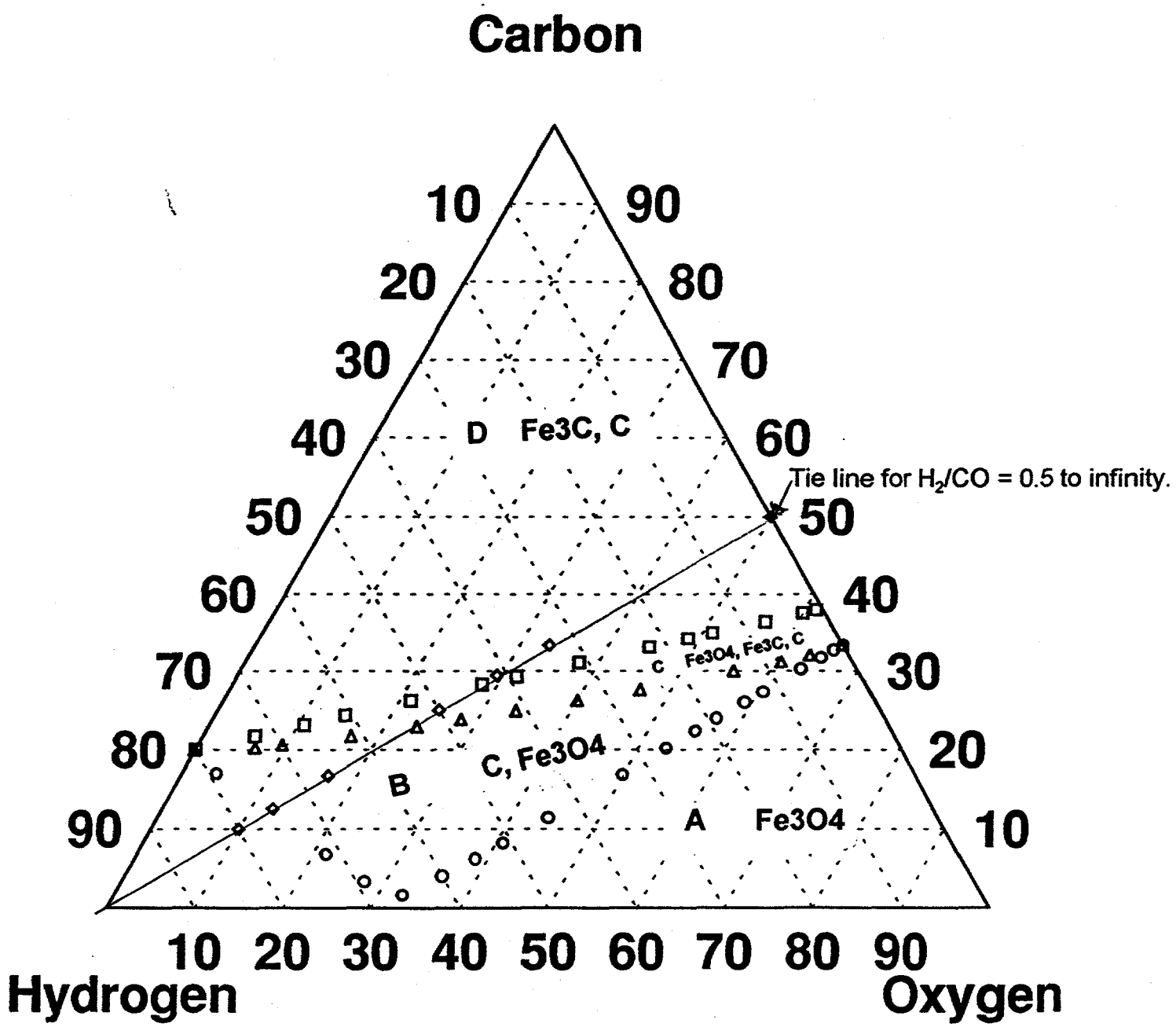

Figure 8. Phase diagram at 15 atm. and 527°C.

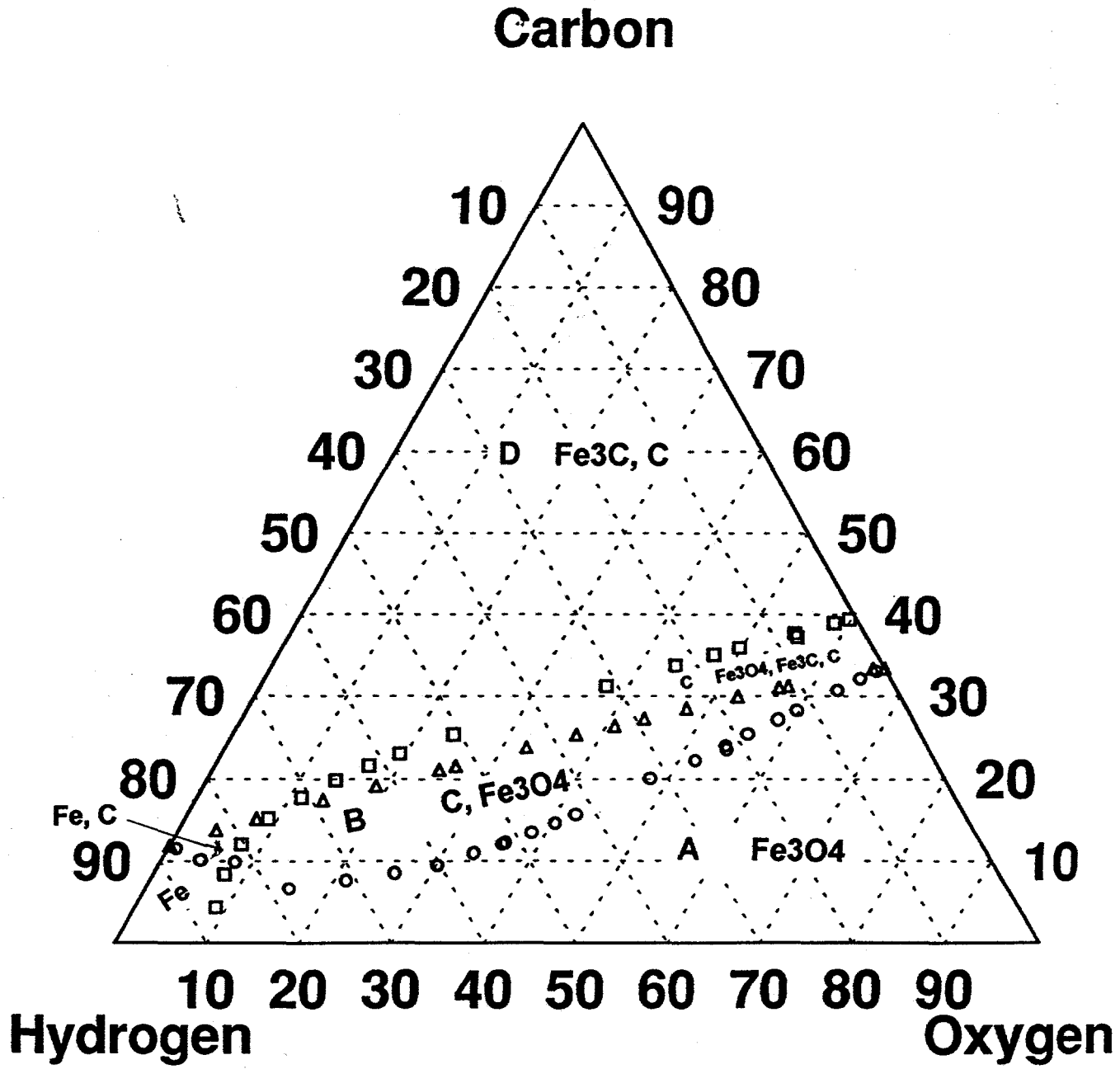

Fig 9

Figure 9. Phase diagram at 15 atm. and 200°C.

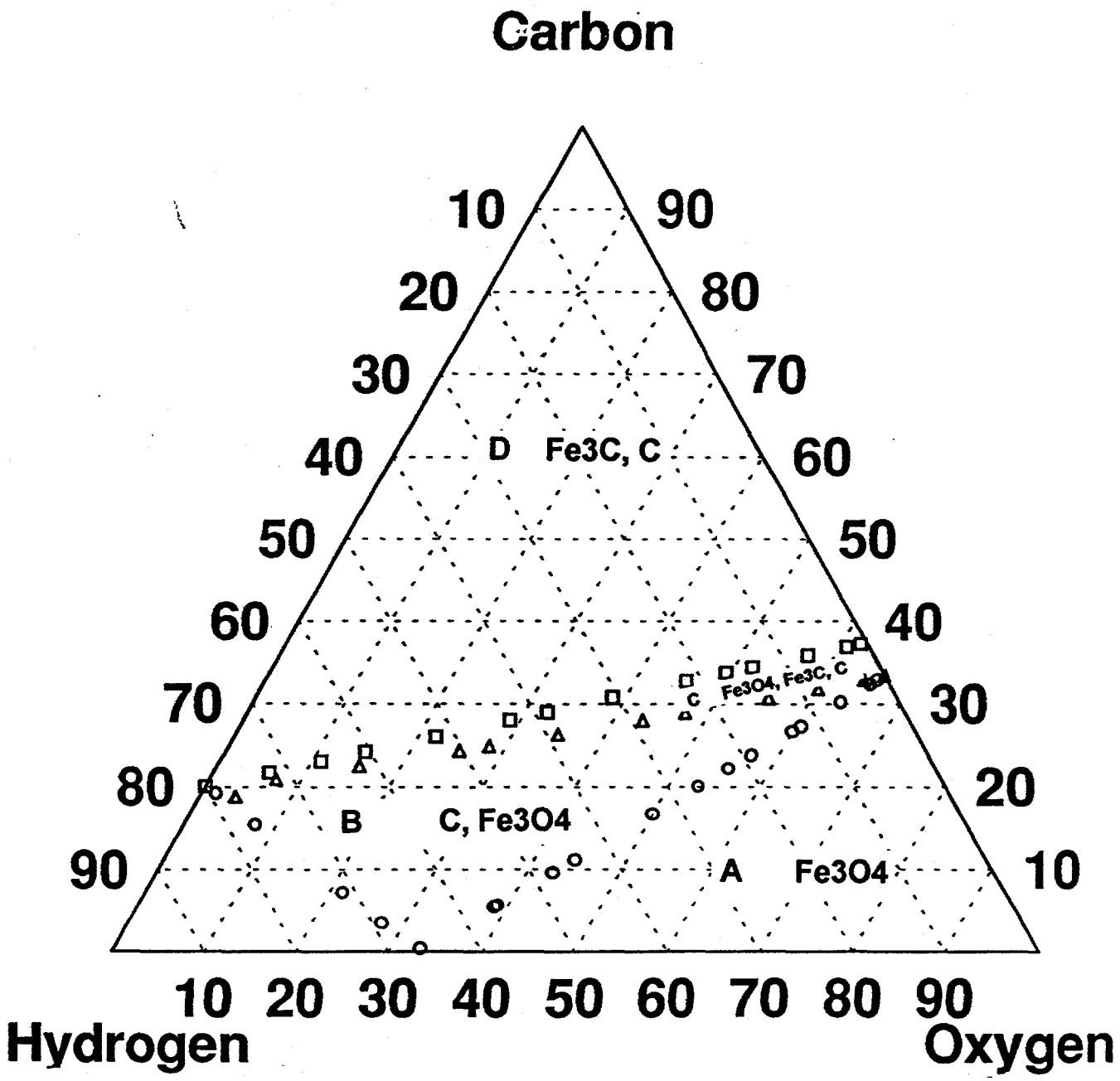

Figure 10. Phase diagram at 15 atm. and 250°C.

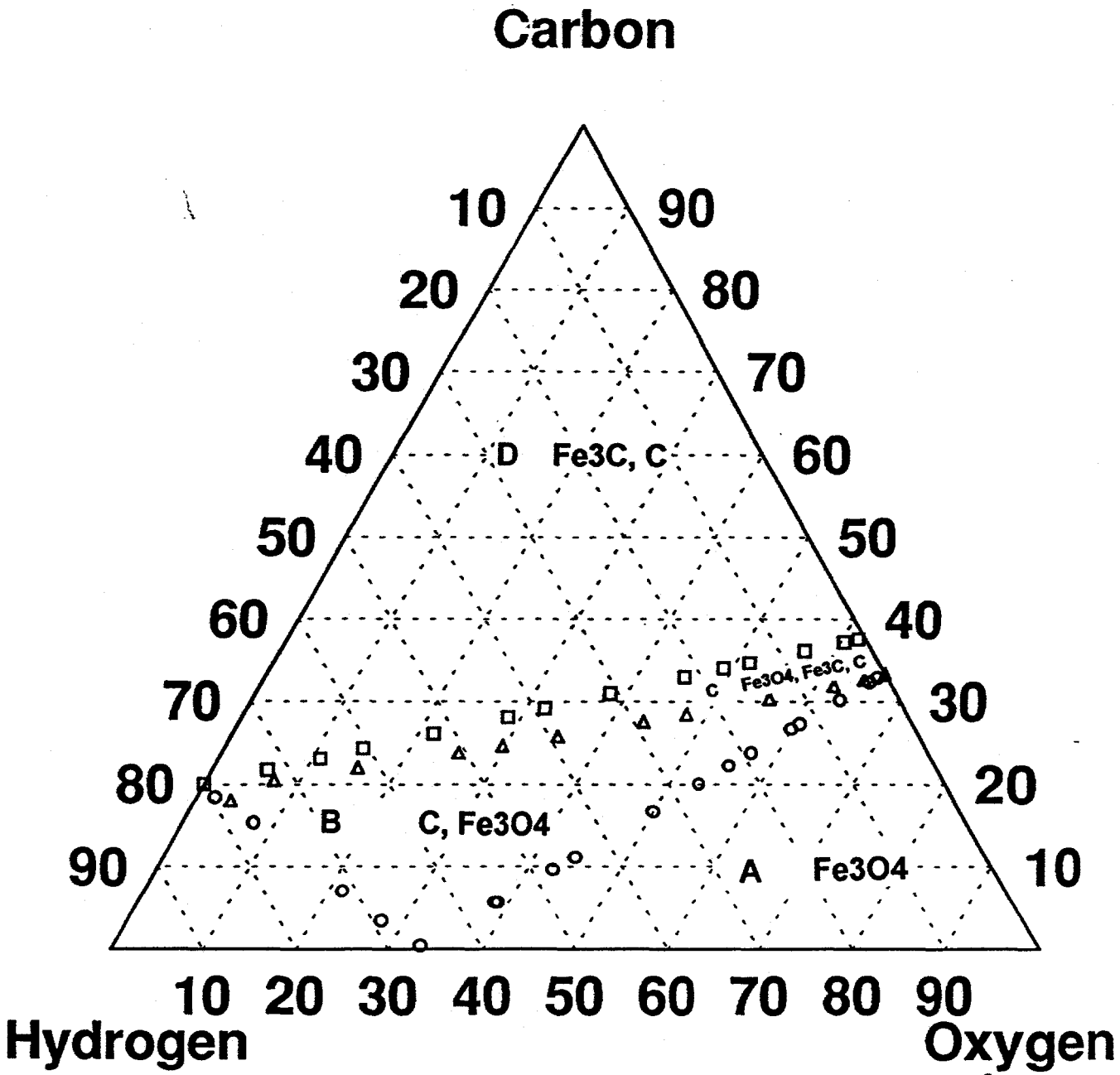

Figure 11. Time needed to convert Fe_3C to Fe_3O_4 at 15 atm. and 300°C. (15 g Fe used : 3.1 NL/hr./g Fe ; X_{CO}=90%).

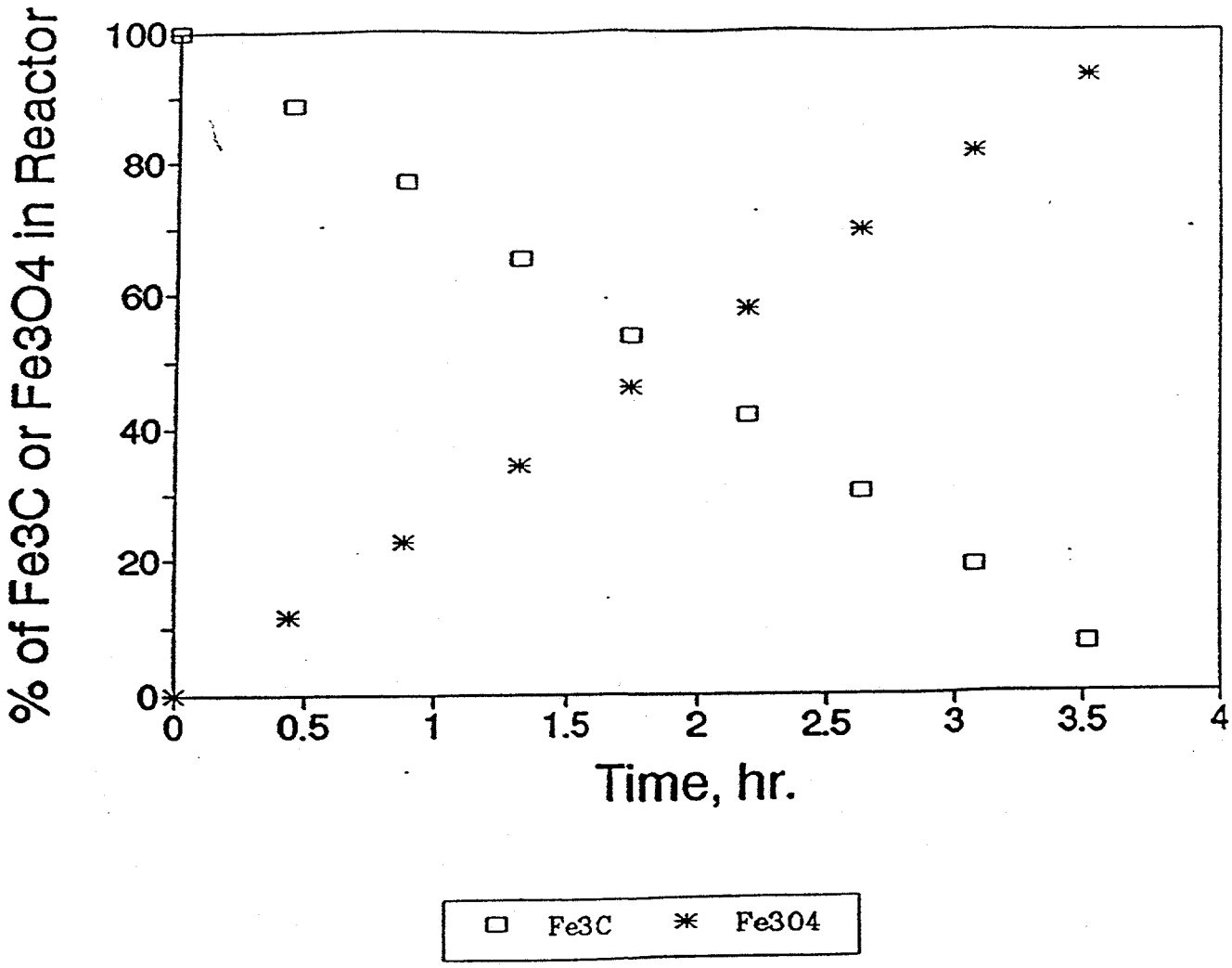

Figure 12.Gas compositions at 15 atm. and 300°C.
(15 g Fe used : 3.1 NL/hr./g Fe ; X_{co}=90%).

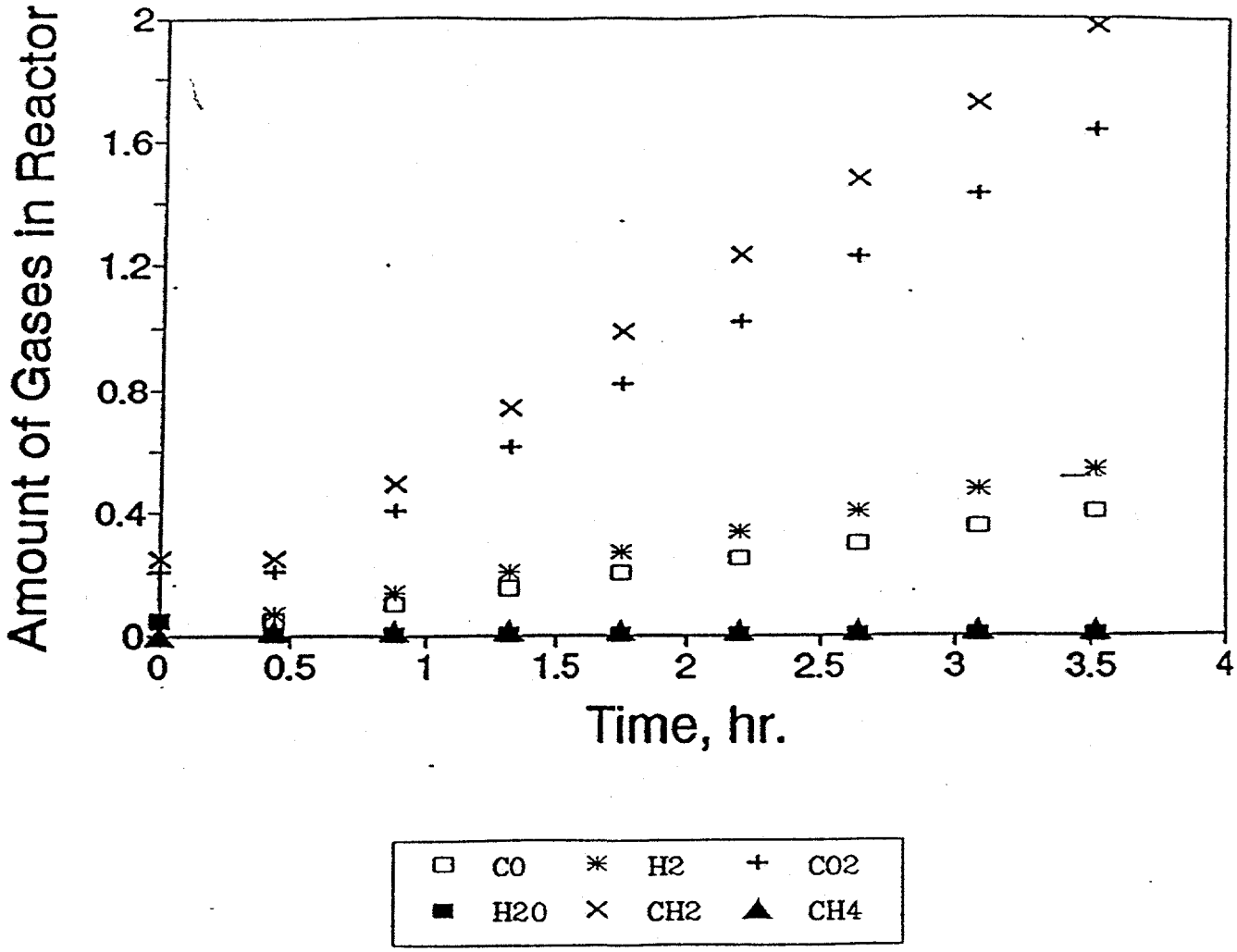

Figure 13.Volume needed to convert Fe_3C to Fe_3O_4 at 15 atm. and 300°C. (15 g Fe used : 3.1 NL/hr./g Fe ; X_{CO}=90%).

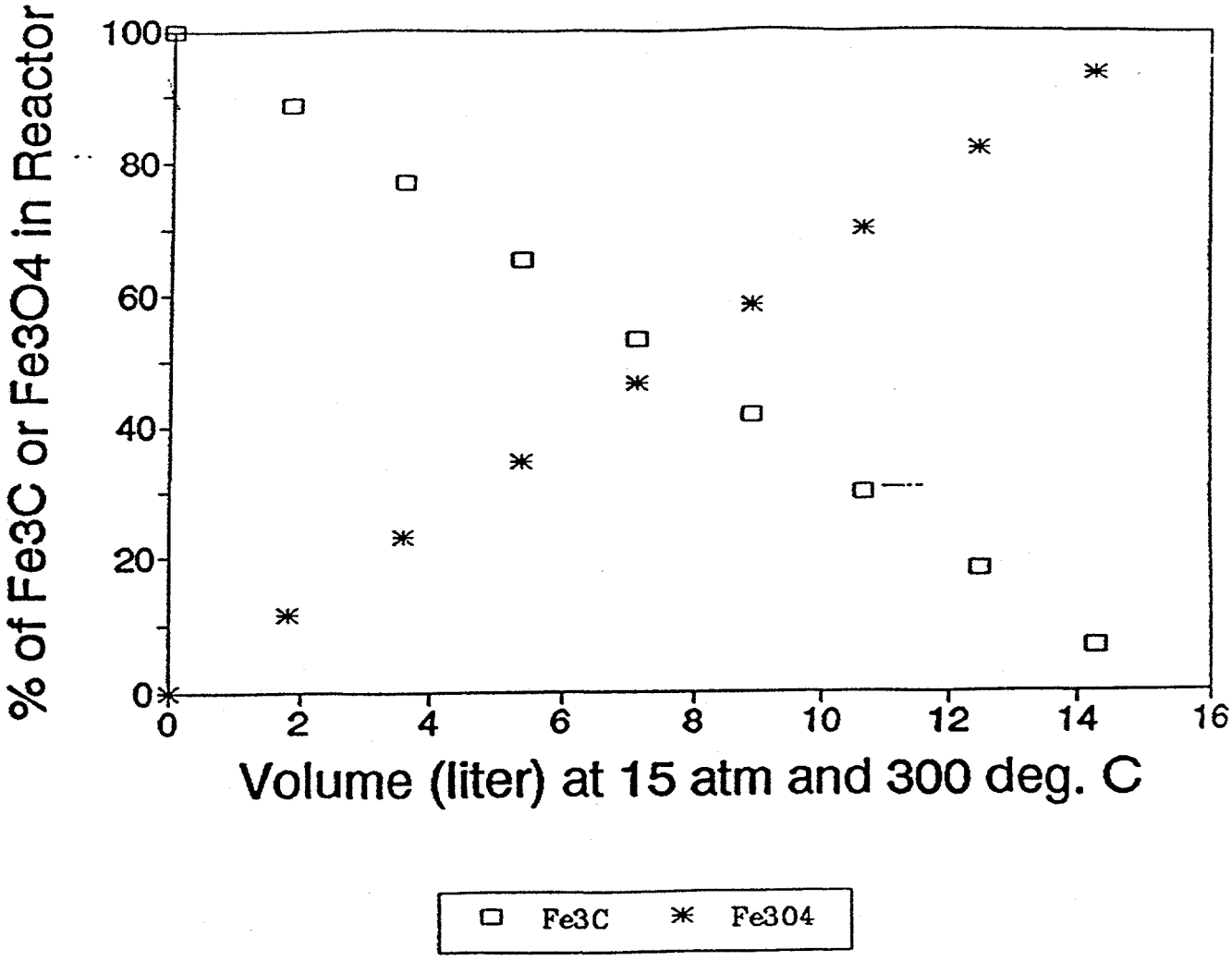

Figure 14.Volume needed to convert Fe_3C to Fe_3O_4 at 15 atm. and 300°C. (15 g Fe used : 3.1 NL/hr./g Fe ; X_{CO}=90%).

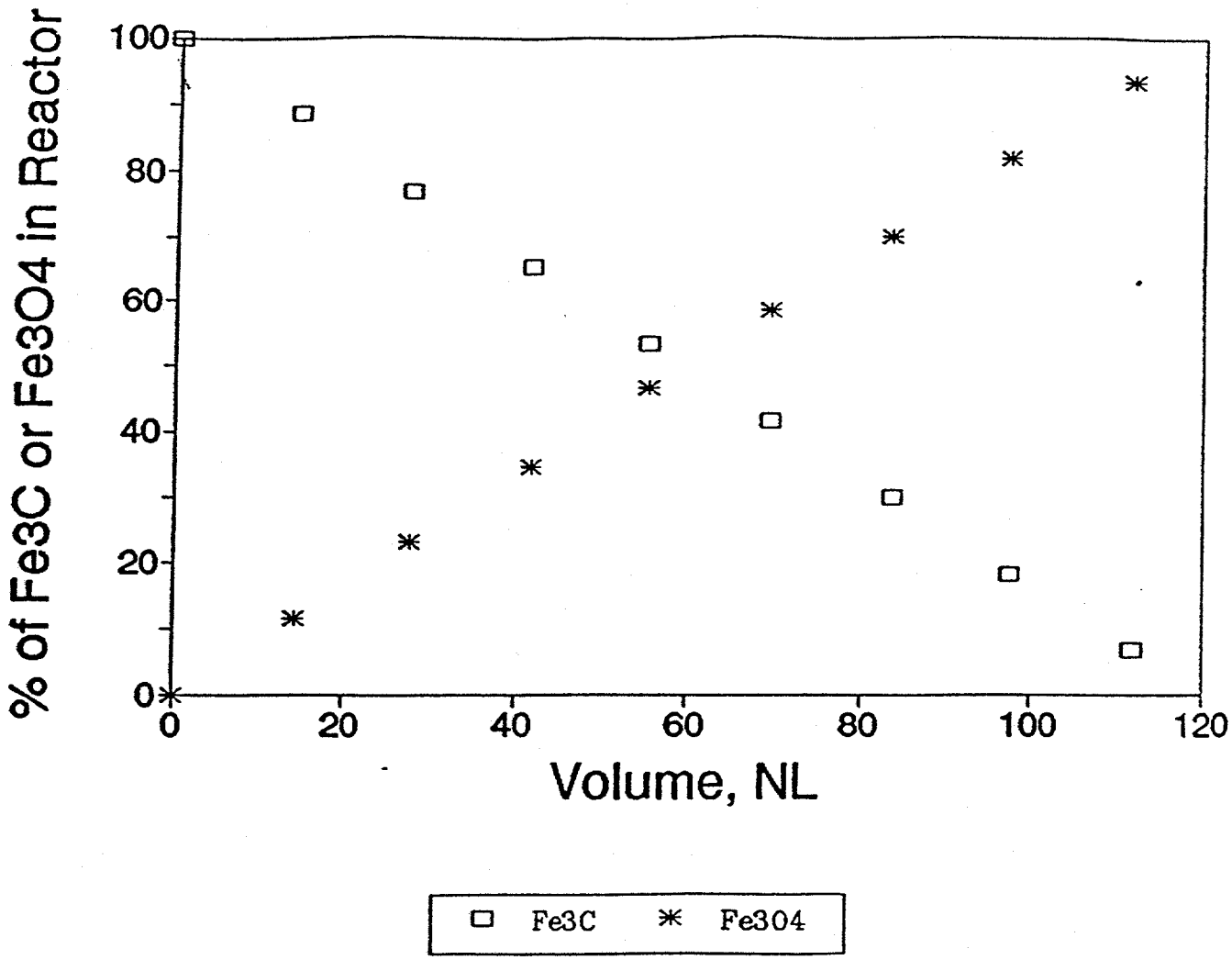

Figure 15. Comparison of experimental data with the calculated phase.

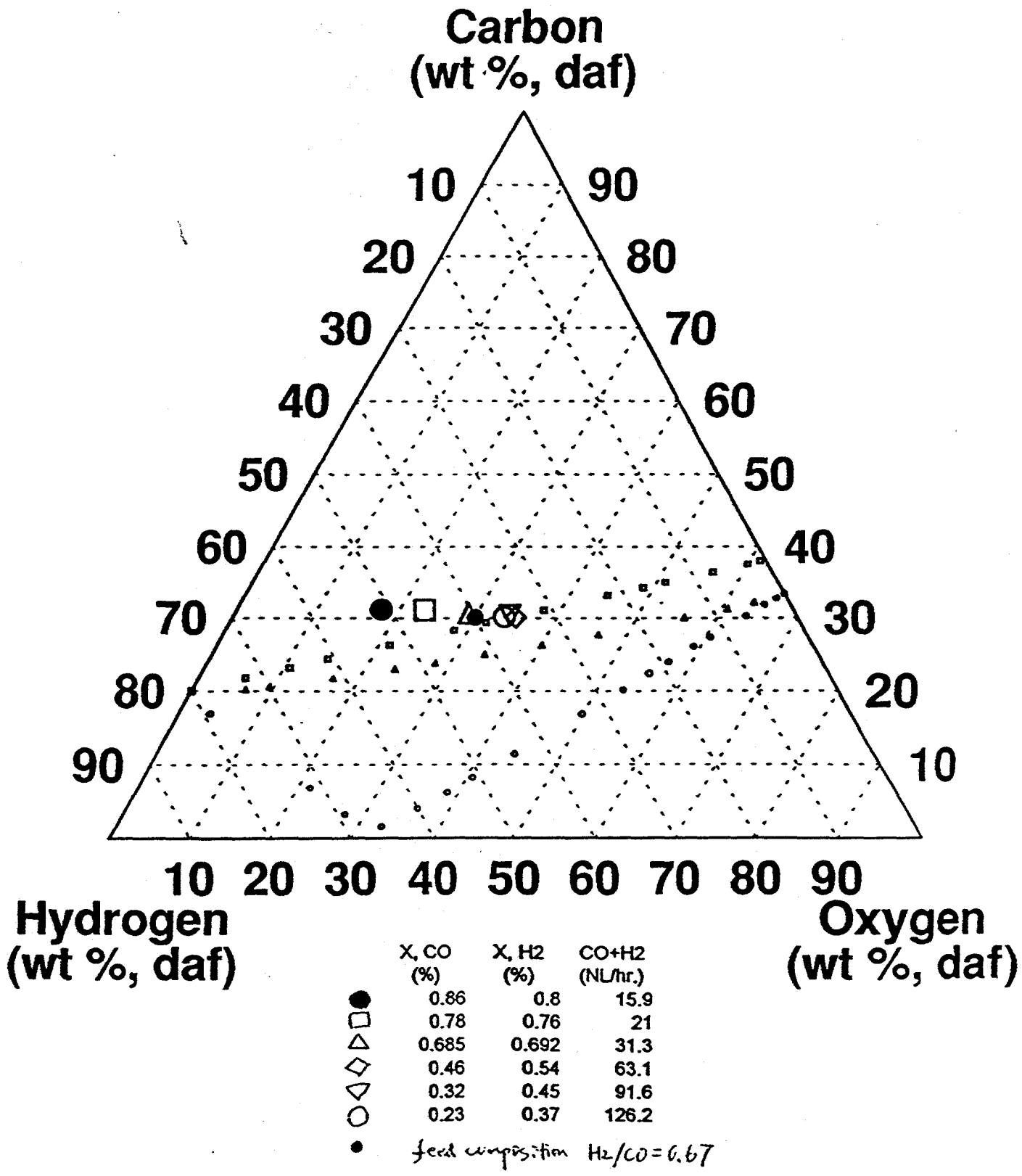

Figure 16. CO and H_2 Conversion with flowrate.

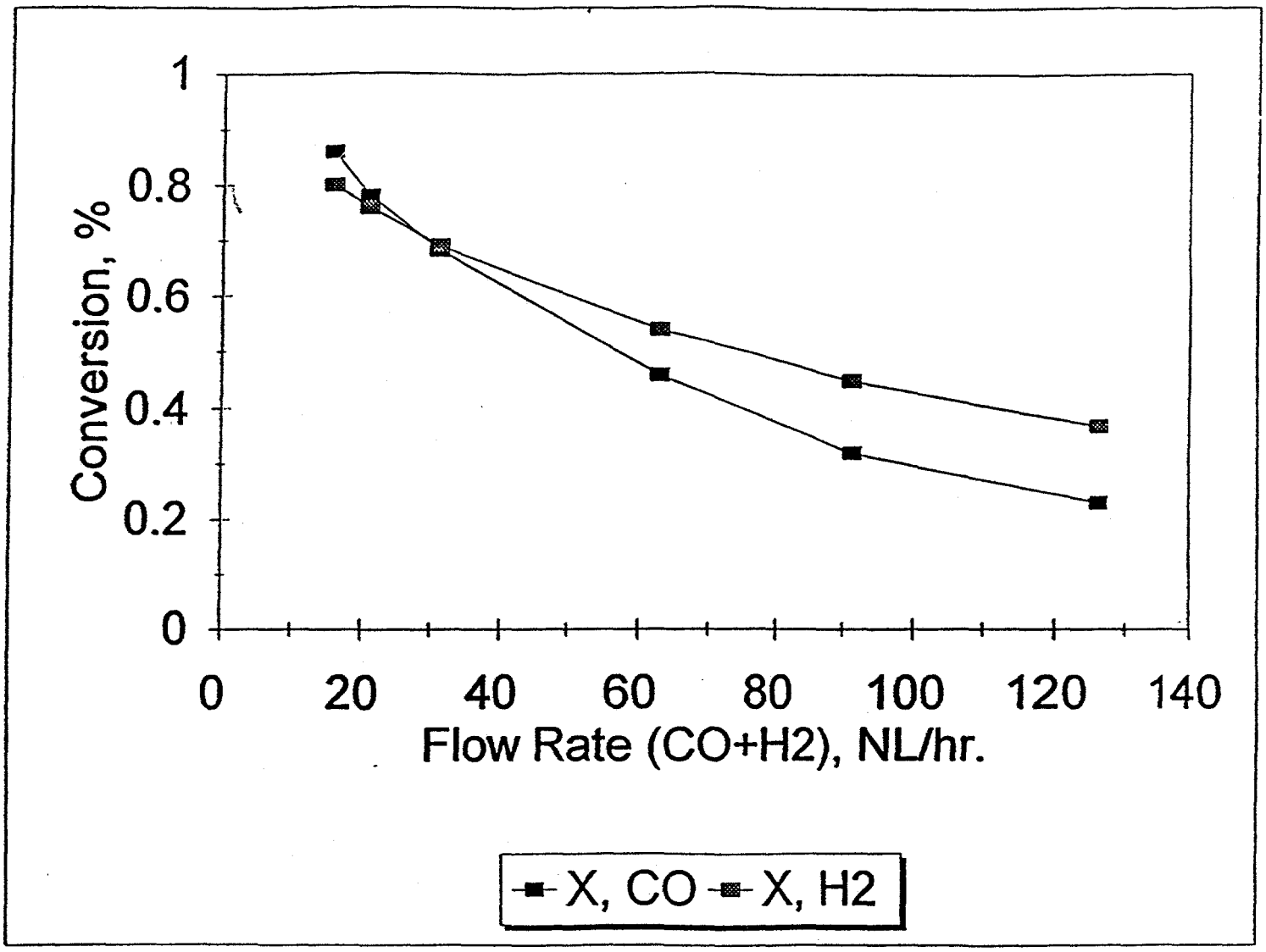

Figure 17. Comparison of the experimental and calculated data in the gas and liquid phases.

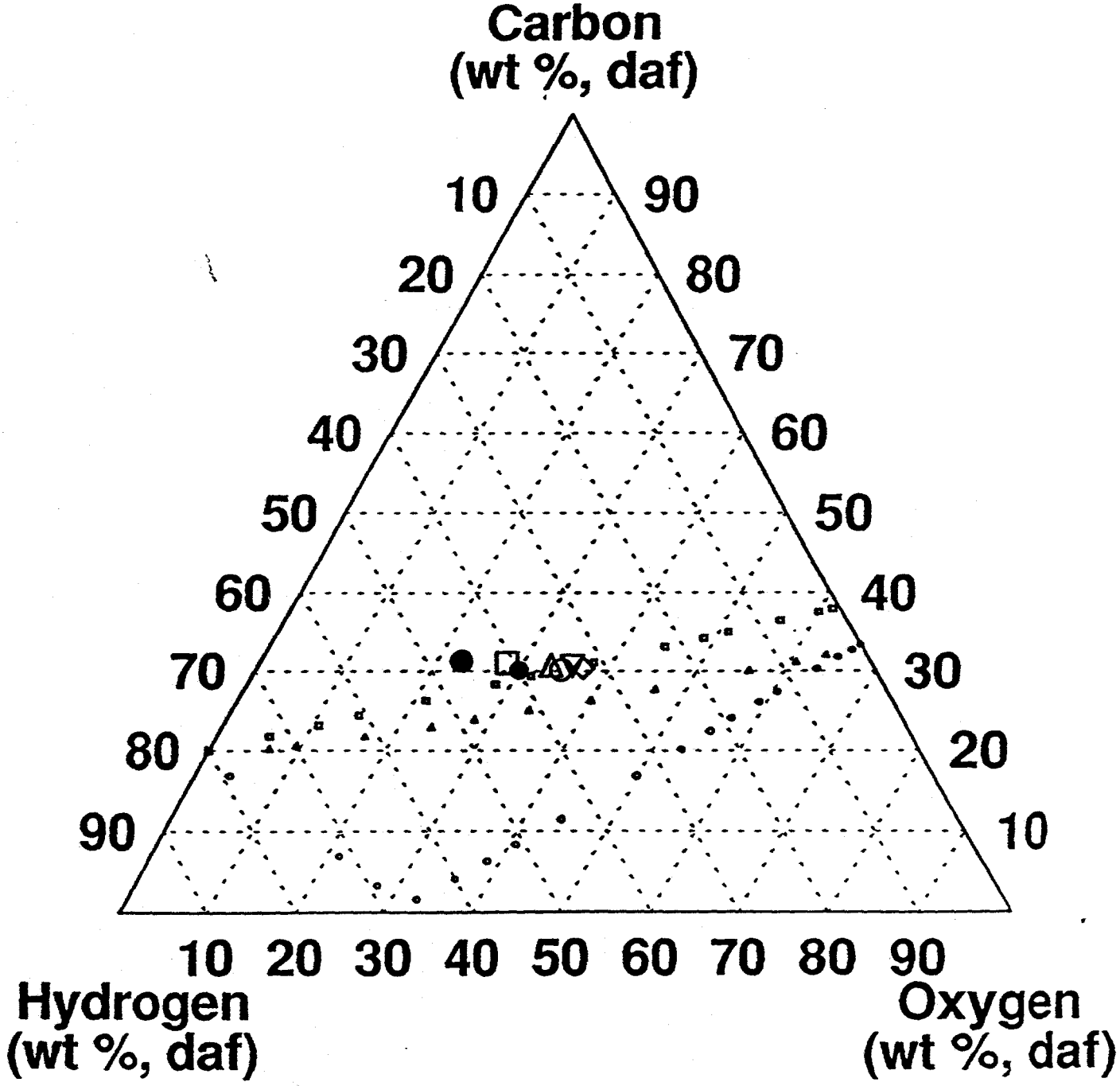

	X, CO (%)	X, H2 (%)	CO+H2 (NL/hr.)
●	0.86	0.8	15.9
□	0.78	0.76	21
△	0.685	0.692	31.3
◇	0.46	0.54	63.1
▽	0.32	0.45	91.6
○	0.23	0.37	126.2
•	feed composition	$H_2/CO = 0.67$	